Relationships of upper tropospheric water vapor, clouds and SST: MLS observations, ECMWF analyses and GCM simulations

Hui Su, Duane E. Waliser, Jonathan H. Jiang, Jui-lin Li, William G. Read, Joe W. Waters

Jet Propulsion Laboratory, Caltech, Pasadena, CA, 91109, USA.

Adrian M. Tompkins

European Center for Medium-Range Weather Forecasts, Reading, UK.

The relationships of upper tropospheric water vapor (UTWV), cloud ice and SST, are examined in the annual cycles of ECMWF analyses and simulations from 15 atmosphere-ocean coupled models which were contributed to the IPCC AR4. The results are compared with the observed relationships based on UTWV and cloud ice measurements from MLS on Aura. It is shown that the ECMWF analyses produce positive correlations between UTWV, cloud ice and SST, similar to the MLS data. The rate of the increase of cloud ice and UTWV with SST is about 30% larger than that for MLS. For the IPCC simulations, the relationships between UTWV, cloud ice and SST are qualitatively captured. However, the magnitudes of the simulated cloud ice show a considerable disagreement among models, nearly by a factor of 10. The amplitudes of the approximate linear relations between UTWV, cloud ice and SST vary up to a factor of 4.

1. Introduction

Variabilities of water vapor and clouds are central to global hydrological and energy cycles [e.g. *Pierrehumbert*, 2002; *Held and Soden*, 2000]. The latent heat release associated with phase transitions among gas, liquid and solid forms of water is one of the main modes of energy transport in the atmosphere. Besides their active roles in moist dynamics, water vapor and clouds both have important radiative effects. The greenhouse effect of water vapor increases sharply when temperature increases, leading to a positive feedback for climate change. Clouds can either warm or cool the Earth's surface depending on their height and thickness. They are also intimately related to the distribution of water vapor, especially in the upper troposphere (UT) [*Lindzen*, 1990; *Betts*, 1990; *Sun and Lindzen*, 1993; *Soden and Fu*, 1995; *Udelhofen and Hartmann*, 1995]. Recent satellite observations of UT water vapor (UTWV) and cloud ice water content (IWC) from the Microwave Limb Sounder (MLS) [*Waters et al.*, 2006] on Aura satellite show that UTWV and IWC are positively correlated, and both quantities increase with increasing sea surface temperature (SST) [*Su et al.*, 2006, hereafter *SU06*]. Over the convective regions, the rate of increase of UTWV with SST is 3 times larger than that for non-convective regions, largely due to the vertical transport of water vapor by deep convection and re-evaporation of condensates [*SU06*]. This convective enhancement of the greenhouse effect by UTWV explains

0094-8276/06/$5.00

roughly 65% of the "Super Greenhouse Effect" [*Raval and Ramanathan*, 1989]. Whether the positive correlations between UTWV, IWC and SST derived from spatial variability of the annual mean data are applicable to temporal correlations of these parameters is on-going investigation. *SU06* termed the positive correlations of water vapor, clouds and SST as "convective UT water vapor feedback" (CWVF). Note that caution needs to be exercised when extrapolating the results regarding feedback mechanisms for long-term climate change.

SU06 provides the first quantitative analysis of relationships among UTWV, IWC and SST using simultaneous direct measurements of UTWV and IWC. It thus serves as a reference point for evaluation of the performance of a state-of-the-art data assimilation model and general circulation models (GCMs) in terms of CWVF. In this paper, we examine to what extent current models capture the relationships of UTWV, cloud ice, and SST as observed by MLS and the magnitudes of the inferred CWVF. We analyze the European Center for Medium-Range Weather Forecasting model (ECMWF) analyses for the same period as the MLS observations, and the mean annual cycles over the period of 1970 to 1999 from a number of GCMs that were contributed to the Intergovernmental Panel on Climate Change (IPCC) 4th Assessment Report (AR4).

2. ECMWF Analyses

We use the ECMWF analyses from the Integrated Forecasting System (IFS) data assimilation system (DAS) for the period of August 2004 to July 2005, same as that for the MLS data in *SU06*. The original 6-hour daily water vapor and IWC profiles are interpolated onto the Aura MLS orbit track in both time and space as developed and described in *Li et al.* [2006]. Then monthly averages are constructed and horizontal re-griding onto the 8° (longitude) $\times$ 4° (latitude) grids is performed, in the same fashion as for MLS data to ensure sampling errors are minimized for comparison.

Figure 1 shows the horizontal maps of annual-mean ECMWF UTWV, vertically integrated between 316 and 147 hPa, and cloud ice water path (IWP) integrated between 215 and 147 hPa. The vertical integrals are constructed in exactly the same way as in *SU06* for direct comparison. The ECMWF IWC at 316 hPa is available but not used because the MLS IWC at 316 hPa is not deemed reliable in current version (v1.5). The resemblance of the spatial distributions of ECMWF UTWV and cloud ice is prominent, while both of them are similar to their MLS counterparts (Fig. 1 in *SU06*). A relatively large difference between ECMWF and MLS data occurs over the continental monsoon regions in South America and Central Africa, where ECMWF UTWV and cloud ice are less than MLS observations. This is likely due to an underestimate of convective intensity over land in the assimilation model [*Li et al.*, 2005]. MLS twice-a-day measurements under-sample the diurnal variability of tropical convection, which may also cause the discrepancy between the analyses and satellite observations. Over the equatorial Inter-Tropical Convergence Zones (ITCZ) in the Pacific and Atlantic Oceans, ECMWF produces less UTWV but more cloud ice than MLS. This may be related to the model's microphysical scheme. Detailed comparison of cloud ice between MLS data and ECMWF analyses is presented in *Li et al.* [2005; 2006]. Here, the focus is on the relationships between UTWV, cloud ice and SST. The approximately linear relations of these quantities are of primary interest.

Figure 2 shows the scatter plots of (a) IWP versus SST, (b) UTWV versus ice and (c) UTWV versus SST, with ECMWF analyses in black and MLS data in blue. Only values over tropical oceans from 30 S to 30 N are used. The monthly SST data are from National Centers for Environmental Predic-

tion (NCEP)/National Oceanic and Atmospheric Administration (NOAA) reanalysis, same as in *SU06*. Different from the scatter plots in *SU06* (their Fig. 2-4), in which annual means are plotted, Fig. 2 uses 12 monthly values from August 2004 to July 2005. Overall, ECMWF and MLS agree with each other quite well. When SST is greater than 300 K, both MLS and ECMWF show that cloud ice increases with increasing SST. In Fig. 2a inset, the increase of cloud ice with SST occurs at similar rate for MLS and ECMWF, with the least squares linear fit slopes of log(IWP) versus SST at 0.71 for MLS and 0.83 for ECMWF. The uncertainties for both linear fits are approximately 5%.

The relationship between UTWV and IWP is shown in Fig. 2b. At the low values of log(IWP) and log(UTWV), where convection is infrequent, the scatter between UTWV and IWP is large. Over the convective regions, the two parameters are strongly correlated, with an approximately linear relationship. The least squares linear fits to MLS and ECMWF data yield similar slopes: 0.17 and 0.21, respectively, with estimated uncertainties around 2% for both datasets.

In Figure 2c, MLS and ECMWF UTWV are plotted against SST, with the least squares linear fits shown separately for SST lower than 300 K and greater than 300 K. For both datasets, log(UTWV) increases with SST at 0.07 per degree when SST is less than 300 K, close to the theoretical value based on the Clausius-Clapeyon equation. When SST is higher than 300 K, the slopes of log(UTWV) versus SST for MLS and ECMWF are 0.19 and 0.26, respectively, with estimation errors around 5%. The larger sensitivity of ECMWF UTWV with SST than MLS may be related to the higher slopes of log(IWP) versus SST and log(UTWV) versus log(IWP) as in Fig. 2a and 2b. Given the uncertainties in estimated regression slopes, the inferred CWVF, as defined in Eq. (1) of *SU06*, is about 30-45% higher in ECMWF than that in MLS data.

3. IPCC 20th Century Simulations

To examine the relationships between UTWV, IWP and SST in state-of-the-art GCMs, we analyze the 20th century simulations from 15 coupled atmospheric-ocean GCMs, which were contributed to the IPCC AR4. Here, we use the mean annual cycles averaged for the 30 year period from 1970 to 1999.

For comparison with *SU06*, the vertical integral of water vapor from 300 hPa to 150 hPa (UTWV) is constructed for all models. The standard outputs of the IPCC runs do not have vertically-resolved IWC. Instead, only tropospheric column-integrated IWP is available. Since most cloud ice occurs in the middle and upper troposphere, the comparison to MLS UT cloud ice is still sensible, with a possible scaling factor. For illustration purpose, both column-integrated IWP and UT IWP for ECMWF analyses are presented in the comparison of the IPCC model results with MLS data. For the analysis of the GCM results, SST simulated from the coupled models is used.

Figure 3 shows horizontal distributions of model-generated annual-mean SST, column-integrated IWP and UTWV for 15 IPCC models. In Fig. 3a, the 300 K SST contours for each model are drawn. They encompass approximately the same areas over tropical oceans. Relatively large model disagreements occur over the eastern Pacific cold tongue, with some models' 300 K contour extending too far east. In Fig. 3b and 3c, the contours of IWP and UTWV at half maximum value for each model are plotted, and the medians of all models are shown in black. The maximum IWP values for all models, ranging from 20 g m^{-2} to 1400 g m^{-2}, are shown in Fig. 3d. Excluding the two GISS models as outliners, the modeled IWP maxima vary by a factor of ~ 10. For references, the maximum column-integrated IWP from ECMWF analyses is 52 g m^{-2}, while the UT (215-147 hpa) IWP for ECMWF and MLS are 12 and 15

g m^{-2}, respectively. Despite the large differences in maximum IWP values, the half-maximum contours are broadly consistent among models. The spatial patterns resemble the tropical convective zones and coincide with the 300 K SST contours. The distributions of the modeled UTWV are quite similar (Fig. 3c). The high UTWV occurs over tropical warm oceans and deep convective regions. The maximum values of UTWV vary from 180 to 450 g m^{-2} (Fig. 3e). The UTWV for ECMWF and MLS are 270 and 310 g m^{-2}, respectively. Near the margins of convective zones, such as south of the equator in the eastern Pacific, inter-model differences are more conspicuous than over the western Pacific warm pool. The among-model differences in the magnitudes of maximum IWP and UTWV (Fig. 3d and 3e) partially confirm previous findings that climate models better simulate water vapor variations than clouds [e.g. *Houghton et al.*, 1995].

The relationships of UTWV, IWP and SST for all models are shown in Fig. 4, and compared to MLS and ECMWF. The 12 monthly data for the mean annual cycles averaged between 1970 to 1999 are used. Only oceanic grid boxes between 20 S and 20 N are considered. In Fig. 4a, log(UTWV) is binned on log(IWP) at an interval of 0.5. In Fig. 4b and 4c, the modeled IWP and UTWV within each 0.5 K SST bin from 290 to 305 K are displayed. To first order, the positive correlations between log(IWP), log(UTWV) and SST are reproduced in the models, with relatively large scatter in log(IWP) and SST relation (Fig. 4b).

The approximately linear relationship between log(UTWV) and log(IWP) is a robust feature for all models (Fig. 4a). Since the modeled IWP is over the entire tropospheric column and larger than that for UT IWP (MLS and EC215), the modeled lines roughly shift to the right with respect to MLS and EC215. The regression slopes for all models and data are similar, around 0.2 to 0.4. Figure 5 shows the ratio of the modeled slopes of log(UTWV) versus log(IWP) relative to the MLS-observed (the blue bars). The differences among the models and data is within a factor of 2. The ratio for MLS is at the constant of one by definition.

In Fig. 4b, IWP stays nearly flat with regard to SST until SST reaches a threshold value, then it increases with SST until another critical point, after which increasing SST is associated with decreasing cloud ice. The threshold SST values for convective initiation vary from model to model, ranging from 295 K to 300 K by subjective estimate of the curvatures in Fig. 4b. The critical SST values for peak IWP vary from 301 K to 305 K among models. The decrease of cloud ice with increasing SST at high values of SST is consistent with previous studies [e.g. *Waliser et al.*, 1993]. It indicates one regime of cloud feedback: clouds act to cool the surface, whereas increasing cloudiness would induce more surface cooling. This negative correlation of IWP with SST is not obvious in the scatter plots (e.g. Fig. 2a) because the number of samples in this high SST range is much smaller than that in lower SST values.

For a quantitative assessment of cloud ice sensitivity to SST in each model, we define the average rate of increase of log(IWP) with SST for individual models as the linear regression slope within 3 K SST range to the left of the SST value at the peak IWP in Fig. 4b. The exact magnitude of the slope depends on the range of SST used; however, the ratio between the modeled and the MLS-observed slopes is found not sensitive to the detailed SST range. Hence, the ratios of modeled regression slopes relative to MLS are displayed in Fig. 5 (the cyan bars). All models, except IPSL, produce a smaller rate of increase of IWP with SST, while ECMWF shows a larger rate, consistent with the results in preceding section. The differences of the ratios among models are approximately by a factor of ~ 4.

Compared to the IWP-SST relation, the log(UTWV) versus SST shows a relatively small divergence among models (Fig.

4c). All models show the increase of UTWV with increasing SST at larger rate when SST is higher. The negative correlation of UTWV with SST occurs at high values of SST, corresponding to the negative correlation of IWP with SST there (Fig. 4b). Similar to the definition of the average rate of increase of IWP with SST, we use the linear regression slopes of log(UTWV) versus SST within 3 K of the SST below the peak UTWV. The ratio of the modeled log(UTWV)-SST slopes relative to the MLS-observed is shown in Fig. 5 (the magenta bars). The ratio varies from 0.5 to 1.5 for the IPCC models, and the ECMWF is about 30-40% larger than the MLS. Overall, the relationships among UTWV, cloud ice and SST are qualitatively re-produced in the state-of-the-art climate models.

4. Conclusions

It is important to quantify the strength of water vapor feedback for climate change predictions. *SU06* used recent satellite observations and found the enhancement of UT water vapor greenhouse effect by tropical deep convection and associated clouds. Here, the relationships of UTWV, cloud ice and SST are examined in the ECMWF analyese and the IPCC model simulations, and a quantitative comparison to the MLS data is presented. The ECMWF analyses agree well with the MLS observations, with about 30% higher sensitivity of IWP and UTWV to SST. For the IPCC 20th century simulations, the magnitudes of the simulated IWP vary considerably among models, nearly by a factor of 10. In the modeled IWP distributions binned on SST, a non-monotonic relationship is shown. Before IWP reaches its peak value, SST appears to be a dominant forcing whereas IWP increases when SST becomes higher. After IWP reaches the peak value, fewer clouds allow more surface warming, and thus a negative correlation of IWP with SST exists at high values of SST. However, the number of samples for this range of SST is quite small. The IPCC models differ by a factor of ~ 4 in terms of the averaged rate of IWP increase with SST. Because of the coupling of UTWV with IWP, the simulated UTWV-SST correlations also yield a sizable deviation, approximately by a factor of 3. The amount of simulated IWP differs by a factor of 10 among models, while the modeled UTWV is more or less consistent in magnitude. The reasons for the model-data discrepancy are likely due to the shortcomings in the physical parameterizations of clouds in the models and improvements can be made when coordinated efforts of combined satellite data and model analysis are underway.

We note that the positive correlations among UTWV, IWP and SST are easier to establish in annual cycle than on any other time scales, such as intraseasonal, interannual or long-term trend, since annual cycle is the most dominant mode in atmospheric internal variability. Whether these relationships are applicable for variabilities on other time scales are yet clear. Nonetheless, our analysis serves as a useful starting point and provides a possible mechanism for future investigation of UTWV variability, its interaction with upper level clouds and their impacts on climate change.

Acknowledgments. This work was carried out at the Jet Propulsion Laboratory, California Institute of Technology, under contract with NASA.

References

Betts, A. K., Greenhouse warming and the tropical water budget, *Bull. Am. Meteorol. Soc.*, *71*, 1464-1465, 1990.

Held, I. M. and B. J. Soden, Water vapor feedback and global warming, *Annu. Rev. Energy Environ.*, *25*, 441-475, 2000.

Houghton, J. J. et al., IPCC Assessment Report, *IPCC Assessment Report*, edited by J. J. Houghton, Cambridge Univ. Press, New York,

1995.

Li, J.-L., D.E. Waliser, J.H. Jiang, D.L. Wu, W.G. Read, J.W. Waters, A.M. Tompkins, L.J. Donner, J.-D. Chern, W.-K. Tao, R. Atlas, Y. Gu, K.N. Liou, A. Del Genio, M. Khairoutdinov, and A. Gettelman, Comparisons of EOS MLS Cloud Ice Measurements with ECMWF analyses and GCM Simulations: Initial Results, *Geosphys. Res. Lett.*, *32*, L18710, doi:10.1029/2005GL023788, 2005.

Li, J.-L., J. H. Jiang, D. E. Waliser, and A. M. Tompkins, Assessing consistency between EOS MLS and ECMWF analazed and forecast estimates of cloud ice, *Geophys. Res. Lett.*, submitted, 2006.

Lindzen R. S., Some coolness concerning global warming, *Bull. Am. Meteorol. Soc.*, *71*, 288-299, 1990.

Pierrehumbert: The hydrologic cycle in deep time climate problems, *Nature*, *419*, 191-198, 2002.

Raval, A., and V. Ramanathan, Observational determination of the greenhouse effect, *Nature*, *342*, 758-762, 1989.

Soden, B. J., and R. Fu, A Satellite analysis of deep convection, upper-tropospheric humidity, and the greenhouse effect, *J. Clim.*, *8*, 2333–2351, 1995.

Su, H., W. G. Read, J. H. Jiang, J.W. Waters, D.L. Wu, and E.J. Fetzer, Enhanced positive water vapor feedback associated with tropical deep convection: New evidence from Aura MLS, *Geophys. Res. Lett.*, *33*, L05709, doi:10.1029/2005GL025505, 2006.

Sun, D. Z., and R. S. Lindzen, Distribution of tropical tropospheric water vapor, *J. Atmos. Sci.*, *50*, 1644-1660, 1993.

Udelhofen, P. M., and D. L. Hartmann, Influence of tropical cloud systems on the relative humidity in the upper troposphere, *J. Geophys. Res.*, *100*, 7423–7440, 1995.

Waliser, D. E., N. E. Graham, and C. Gautier, Comparison of the highly reflective cloud and outgoing longwave radiation datesets for use in estimating tropical deep convection, *J. Clim*, *6*, 331–353, 1993.

Waters, J. W., et al., The Earth Observing System Microwave Limb Sounder (EOS MLS) on the Aura satellite, *IEEE Trans. Geosci. Remote Sensing*, *44*, 1075-1092, 2006.

Hui Su, Jet Propulsion Laboratory, California Institute of Technology, Pasadena, California, 91109, USA. (Hui.Su@jpl.nasa.gov)

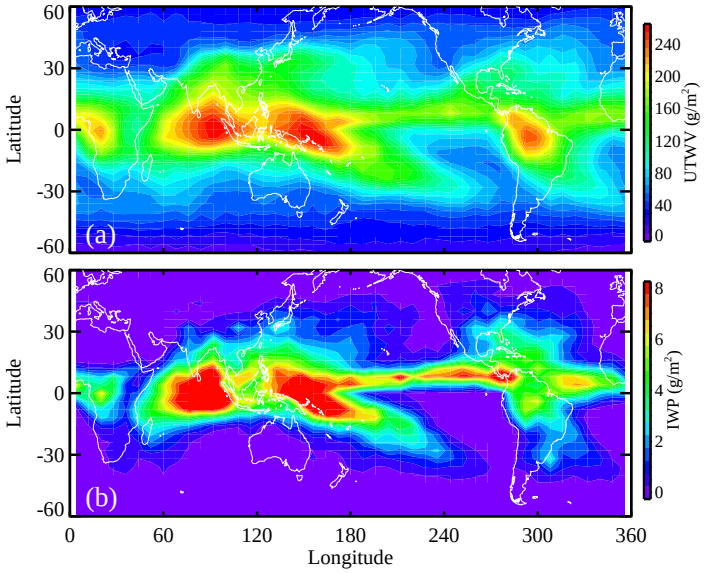

Figure 1. Maps of annual mean ECMWF (a) UTWV (vertically integrated from 316 to 147 hPa) and (b) IWP (vertically integrated IWC from 215 hPa to 147 hPa).

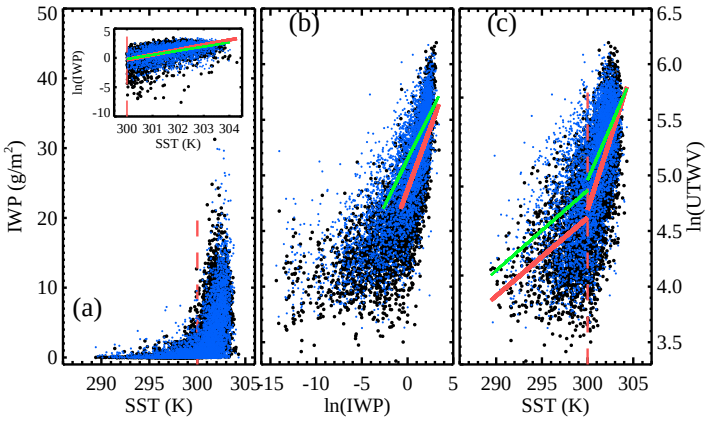

Figure 2. Scatter plot of MLS-observed (in blue) and ECMWF analyses (in black) (a) IWP versus SST, (b) UTWV versus IWP, both in natural logarithmic scale, and (c) log(UTWV) versus SST. The inset in (a) shows the scatter plot of the log(IWP) versus SST for SST $\geq 300K$. Each point corresponds to a monthly mean from August 2004 to July 2005 in the $8^\circ \times 4^\circ$ oceanic boxes within 30S-30N. The red and green lines are the least squares linear fits to the ECMWF and MLS data, respectively.

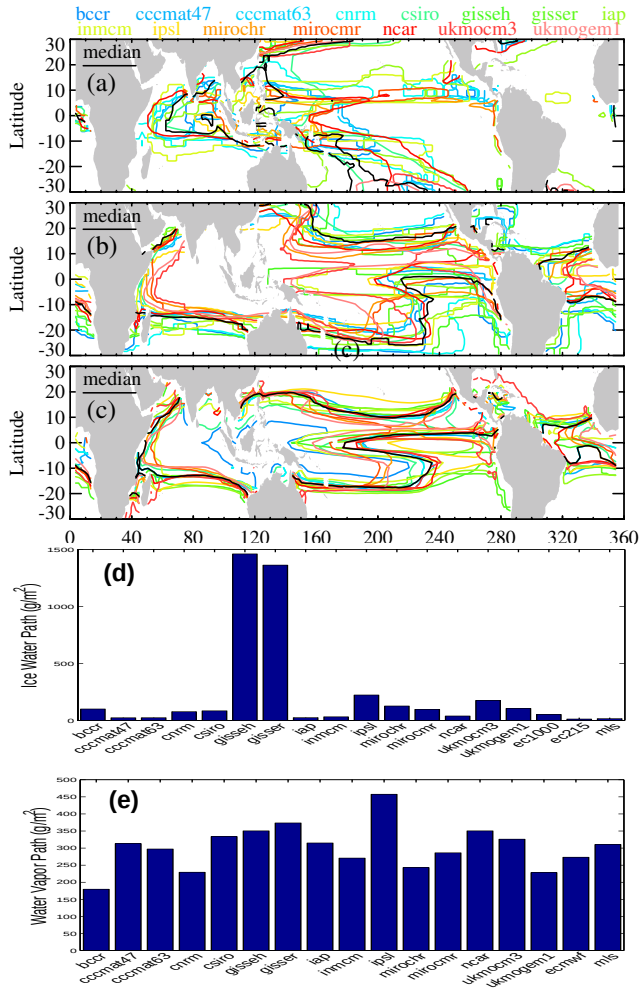

Figure 3. Maps of IPCC simulated annual mean (a) SST (contoured at 300 K), (b) IWP and (c) UTWV (both contoured at 50% of respective maxima) over the period 1970-1999, and the maximum values of (d) IWP and (e) UTWV for each model, in comparison to the ECMWF and MLS. EC215 denotes the UT IWP integrated from 215 hPa and up. EC1000 denotes the column-integrated IWP. In (a), (b) and (c), each model corresponds to one color, with the median of models shown in black.

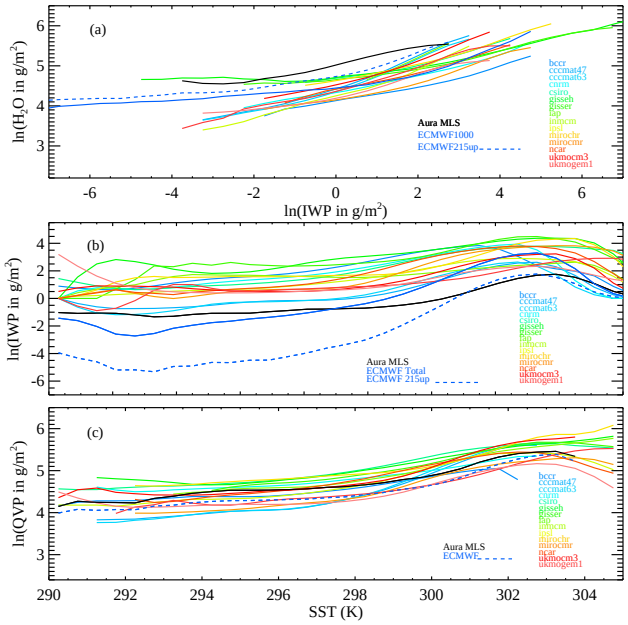

Figure 4. Distributions of (a) log(UTWV) in each 0.5 bin of log(IWP), (b) log(IWP) and (c) log(UTWV) in each 0.5 K bin of SST for the IPCC models along with the ECMWF and MLS. ECMWF215up denotes the UT IWP integrated from 215 hPa and up. ECMWF1000 denotes the column-integrated IWP.

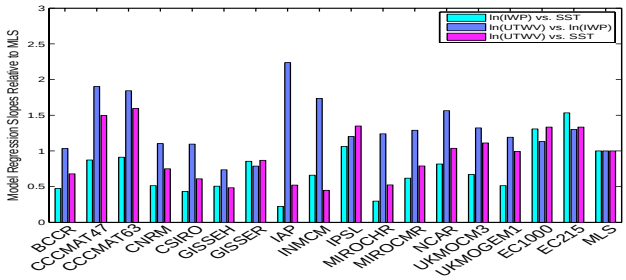

Figure 5. The ratio of the regression slopes of log(IWP)-SST, log(UTWV)-log(IWP), and log(UTWV)-SST relative to the MLS-observed for the IPCC models, ECMWF and MLS.